International Journal of Innovative Computing, Information and Control
Volume **8**, Number **3(B)**, March **2012**

ICIC International ©2012 ISSN 1349-4198
pp. 2101–2112

THE ACTIVE CONTROL DESIGN FOR DMFC/BATTERY HYBRID SYSTEM USING PIDNN

Chi-Yuan Chang[1,3], Chao-Hsing Hsu[2], Wen-June Wang[1] and Charn-Ying Chen[3]

[1]Department of Electrical Engineering
National Central University
No. 300, Jungda Rd., Jhong-li, Taoyuan 32001, Taiwan
benny@iner.gov.tw; wjwang@ee.ncu.edu.tw

[2]Department of Computer and Communication Engineering
Chienkuo Technology University
No. 1, Chieh Shou N. Rd., Changhua 500, Taiwan
hsu@ctu.edu.tw

[3]Institute of Nuclear Energy Research
No. 1000, Wenhua Rd., Jiaan Village, Longtan, Taoyuan 32546, Taiwan
cychen@iner.gov.tw

Received December 2010; revised April 2011

Abstract. *This paper presents a PID neural network (PIDNN) controller designed for a direct methanol fuel cell (DMFC)/Battery hybrid generation system. To maximize the power produced by the DMFC stack in stable operation, high loading with batteries is employed for balancing power flow. Keeping the power produced by the DMFC stack at high efficiency with low loading prevents the problem of methanol crossover. In consideration of the characteristics of DMFC stack during actual operation, we use a bidirectional DC/DC converter connecting the battery to the DC bus to manage the power distribution between the fuel cell and the battery. PIDNN control allows for adequate pulse-width modulation (PWM) control of the bidirectional DC/DC converter with fast response, increases the transient performance of the DMFC fuel cell system and satisfies the requirement of energy management. The active control is designed to achieve the abovementioned multiple objectives. To verify the reliability and stability of the proposed control, an experiment was performed; the results show that the proposed control can efficiently achieve the multiple objectives.*
Keywords: DMFC, Active hybrid control, PIDNN, Bidirectional converter

1. **Introduction.** Fuel cells have been widely studied and are considered to constitute a promising future alternative power source due to the increasingly critical energy crisis as well as environmental concerns. Fuel cells have shown promising potential for many possible applications such as in portable electronics, hybrid electric vehicles, remote telecommunication facilities and remote ground support stations for light vehicles, [1-3]. Early developers mainly focused on hydrogen-feed polymer-electrolyte fuel cells (PEMFC) but recently, direct methanol fuel cells (DMFCs) have attracted more and more attention due to their advantages. Since the liquid methanol solution is a feed without the need for any reformer, the system design can readily be made available for consumers. Moreover, in a comparison with PEMFC, the use of a liquid methanol solution can avoid the problems of complex humidification and thermal management in the system design [4-6]. As a result, many research institutes and universities are targeting their efforts at the integration of DMFC into small electrical appliances. However, there are some problems, such as

methanol crossover, low catalyst activation and less durability, which continue to restrict the commercialization of the DMFC system.

Although the DMFC has the potential to be developed into a portable power source, the main drawbacks, which include the long start-up time and poor response to transient power demand, limit the practical applications. In order to improve on these drawbacks, a hybrid power configuration consisting of a DMFC stack and batteries is proposed. The method provides the required power to each device during the actual operation. However, this passive hybrid has a number of disadvantages. First, it is necessary to match the normal voltage of the DMFC stack to that of the battery by eliminating much of the flexibility in the system design. Furthermore, because the power depends on the characteristics of each component being passively distributed between the fuel cell and the battery, the maximum output current of the hybrid system might be reduced by the activity of the fuel cell. Therefore, an actively controlled DMFC/battery hybrid method was published in [7-9]. This design can be scaled to larger or smaller power capacities for a variety of industry applications. Moreover, in seeking to satisfy adequately high peak power demand to the load, a hybrid fuel power supply with rapid dynamic response was investigated. The proposed hybrid power supply features include both high peak-power capacity and fast response to the load power change [10]. Also, the DMFC stack in parallel or series, with the batteries as the hybrid power sources, was investigated in actual operation. The stack ideally should be operated at the point of high efficiency. However, those abovementioned hybrid forms have no active control to keep the stack reacting at the best operating point. Therefore, the voltage of the DMFC stack needs to vary according to the power demands. The DMFC stack demanded for long-term operation may run in the diffusion region as the load power is very high. Furthermore, at a low load operation, the DMFC stack will run with less efficiency, causing the problem of more methanol crossover with a constant methanol flow [11-15]. Then, the hybrid system control methodology of the two power sources must be determined. Numerous studies discuss the system architecture and control design of the fuel cell and battery (or ultracapacitor) hybrid system. However, few papers focus on the DMFC hybrid system. [16-20] analyzed the performance of a hybrid DMFC and battery hybrid system, but its hybrid control was passive and simple, without considering the DMFC and battery protection, and with no active load sharing. Therefore, there is a great demand for a novel design of DMFC hybrid EMS with simple but effective hybrid control and complete DMFC and battery protection. The target system must be able to avoid any accidental damage to the DMFC, provide fast dynamic load and exhibit improved performance.

This paper is organized as follows. In Section 2, a general description of the architecture and the principle of a DMFC system and hybrid power setup is presented as well as a designed bidirectional Converter for the system. In Section 3, the control strategies of the DMFC stack are discussed and conducted in addition to a control theory offered for the PIDNN design concept. In Section 4, the experiment results are discussed and a comparison made of the proposed controls. Finally, some conclusions are offered in Section 5.

2. DMFC for Hybrid System.

2.1. DMFC system. In this work, the Johnson Matthey Nafion 115 membrane electrode assembly (MEA) is employed for the DMFC stack configuration. The active area of MEA is 50 cm^2 in which the Pt-Ru loading is 2 mg/cm^2 and Pt loadings is 2.5 mg/cm^2. The 12-cell DMFC stack is built from the above MEAs, designed and fabricated with conventional bipolar plates and parallel serpentine flow fields [21,22] carbon cloth, gaskets and machined

graphite bipolar plates. The MEA is sandwiched between carbon papers and then installed into a bipolar plate stack with two current collectors positioned at each end of the stack. Teflon gaskets are placed between bipolar plates to prevent liquid and gas leakage to the exterior and/or cross leakage between the fluids in the stack. Serpentine type flow fields are used for fuel distribution on the anode and cathode sides. Finally, the current collectors are made from stainless steel or titanium alloy. The gasket thickness of both the anode and cathode sides is 0.2 mm. The power performance of this stack with a 3.0 wt.% methanol concentration at 60° is shown in Figure 1. The maximum power output is 35 W at 6 V.

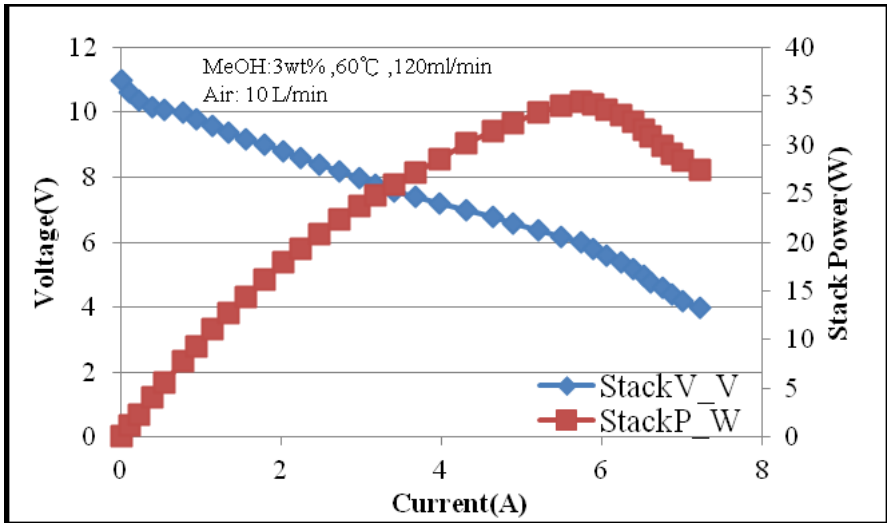

FIGURE 1. DMFC stack polarization curve

2.2. **Analysis and design of hybrid setup.** A hybrid fuel cell/battery power device consists of a DMFC stack, a number of rechargeable batteries and a DC/DC converter controlled by a programmable device. There are many existing hybrid configurations in the literature [27-30]. Generally there are two types of hybrid setups: Passive and Active hybridization. Passive hybridization means that two energy sources are directly connected to the load (or through a diode or MOSFET) without any active and dynamic power conditioning. The active hybridization is more advanced compared to passive hybridization since either fuel cell, battery or both outputs are controlled to adjust the load sharing between two sources. Figure 2 is a simple proposed passive hybrid architecture [23]. The diode can prevent the fuel cell from reverse charging. However, this hybrid configuration is not within our consideration since the fuel cell cannot tolerate reverse charging current.

The maximum fuel cell current is determined by I-V curves of fuel cell and battery. When the load current is larger than the maximum fuel cell current, the fuel cell voltage will drop below the battery voltage so that diode D2 will be turned on. The fuel cell will continue to output maximum current and the battery will provide the remaining current. The diodes work as a "logic" source; otherwise, the energy source with higher voltage will be selected for load supply. As depicted in Figure 1, the classical power conservative law (without losses) of the DMFC/Battery hybrid power source is as follows:

$$P_{load}(t) = P_{DMFC\,Stack}(t) + P_{Battery}(t) \tag{1}$$

where P_{load} is the load power, $P_{DMFC\,Stack}$ is DEMC stack output power and $P_{Battery}$ is battery supply power.

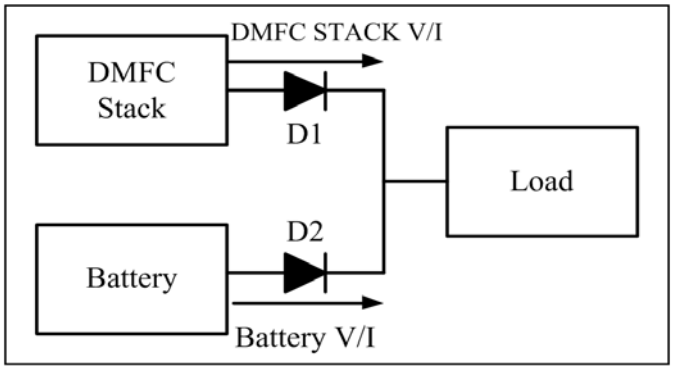

FIGURE 2. Simplest passive hybrid architecture

The advantages of this hybrid configuration are its simplicity, cost effectiveness, lack of complicated control and the entire load sharing being accomplished passively. The problem with this architecture is the varied maximum fuel cell current. With the discharge of the battery, the battery voltage will vary and thus the maximum current that the fuel cell can provide may change as well, precluding battery protection; battery overcharging/discharging and overcurrent protection cannot be implemented with this hybrid configuration. A separate charging circuit is needed for battery charging since the battery current can only be unidirectional. The fuel cell is not a stand-alone component and is instead connected to another power generation device, such as a battery; a thorough control of the power supply becomes necessary. For this purpose, we insert a DC/DC converter in a battery series in our design so that the battery output voltage will be controlled (Figure 3).

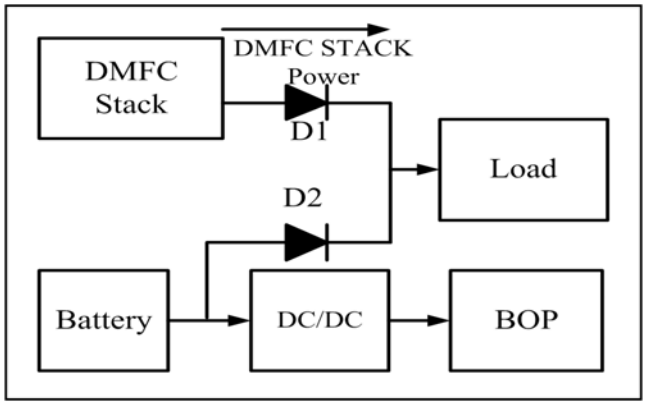

FIGURE 3. Half active hybrid with BOP and load

Hence the fuel cell maximum output power can be fixed or limit, as shown in Figure 4. The merit of this architecture is controllable maximum fuel cell current. Also since the battery output voltage is regulated, its output can be used as the auxiliary power supply for some BOP components, such as circulating pump or air blower fan. But again, since battery charging is not available, battery charging must be implemented using a separate battery charging circuit.

We then designed a bidirectional converter (c.f. the 2 quadrant chopper), so that the battery discharging/charging can be controlled dynamically. In this hybrid configuration, the battery current can work in both directions, and be adjusted by controlling the duty cycle of the bidirectional DC/DC converter. One diode is needed between the fuel cell and load to block the reverse current, and the fuel cell current is limited by dynamic

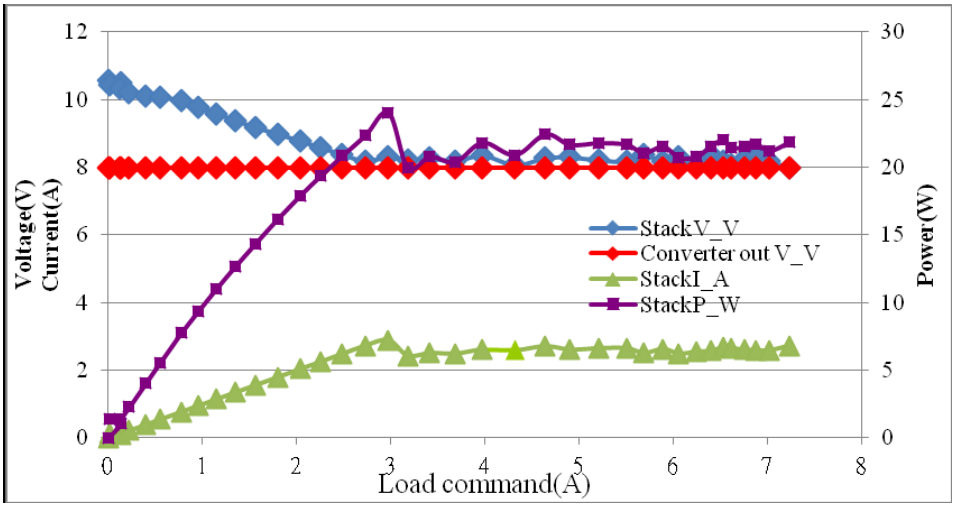

FIGURE 4. Fuel cell and battery I-V curves with battery voltage regulated

control of battery current. A Buck-Boost Converter, or 2-quadrant chopper, is widely used for this application, as shown in Figure 5. Many references can be found for this hybrid architecture and most of them are designed for DMFC/battery or hybrid system.

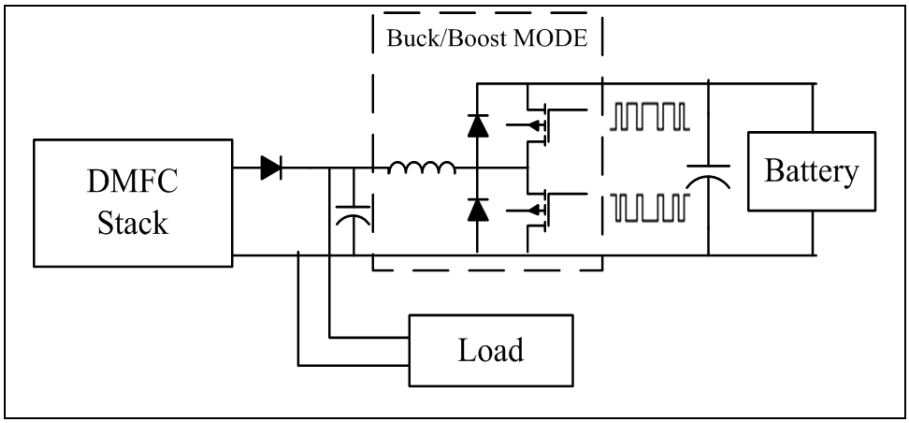

FIGURE 5. Bidirectional converter for active hybrid

The advantages of this configuration are: management of battery discharging and charging, and the battery current is directly controlled by the bidirectional converter so that the battery over discharge/charge and overcurrent protection can be implemented. The fuel cell current can be limited. Although the fuel cell current is not controlled directly, it can be limited by adjusting the battery current. Also, the diode can prevent reverse current flow; no separate battery charging circuit is needed. The battery current now can be controlled to flow into the battery and no additional battery charging circuit is required.

2.3. **Experimental setup.** In the work presented in this paper, the hybrid power supply system is comprised of a DMFC fuel cell stack, a lithium ion battery, and a bidirectional converter controlled by a programmable device, which are connected to the same voltage bus through appropriate converters and controls. The block diagram of the experiment setup is shown in Figure 6. The specifications of DMFC are including nominal power capacity 35 W and nominal open-circuit voltage with 11 V. In this configuration, the

nominal output voltage of hybrid power device is 8 V. Furthermore the variables of configuration are defined as following. The $V_{FC}(t)$ is the voltage of DMFC stack, $I_{FC}(t)$ is the current of DMFC stack, $V_{Battery}(t)$ is the voltage of battery, $I_{Battery}(t)$ is the current of battery, $V_{Load}(t)$ is the voltage of load and $I_{Load}(t)$ is the current of load. The control code was executed on a general-purpose DAQ control board (Model DIO9401 NI) via the onboard A/D converters. The control algorithm was first computed in the PIDNN control and then downloaded to the DAQ control board. The operating condition, such as the currents and voltages of the fuel cell and the battery are monitored and fed to controller, which is used to coordinate bidirectional converter. The power conditioning system (including power converters and controls) controls the voltage of each component, and allocates the available power to recharge the battery if possible.

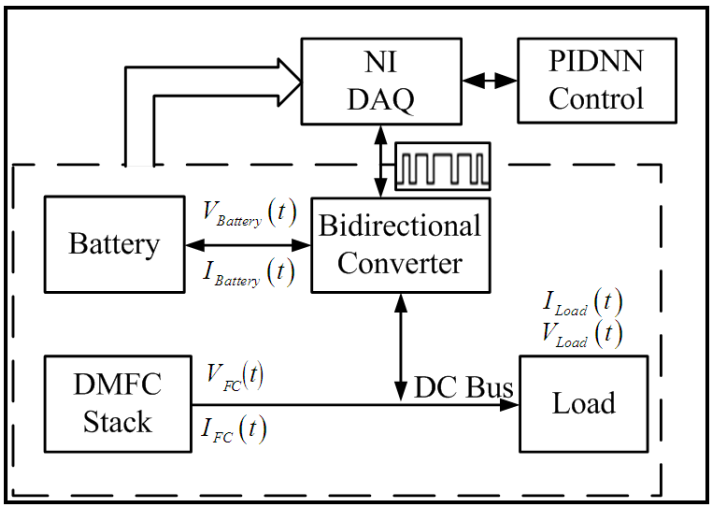

FIGURE 6. Block diagram of the experiment setup

3. Control Strategies of Hybrid DMFC System.

3.1. **PIDNN control concept.** Due to the nonlinear essence and excellent ability of function approximation, an artificial neural network (ANN) is introduced into the control field for the controller design [24-26]. However, ANN-based controllers are not used widely in the control field since neurons in most neural networks only display a static function; this is not suitable for the control of an actual dynamic system [27]. In view of the good dynamic performance of PID and the merits of an artificial neural network, SHU Huailin [28] first proposed P, I, D neurons and designed a PID neural network (PIDNN). Instead of being a simple hybrid system of the PID and neural network, PIDNN is actually a new kind of dynamic neural network. Some PIDNN-based controllers were designed to control linear or nonlinear systems and achieved better control performances [29-31]. The training algorithm for the above controller design is a conventional BP algorithm; the training results are greatly influenced by the initial values and learning rate. The ability of global exploitation is not strong and easy to maintain within the local minimum [32,33]. The BP algorithm constrains the wide application of the PIDNN controller. PIDNN, which is present in a new kind of network, and its hidden layer neurons simply work as a PID controller through their active functions; thus, it simultaneously has the advantages of both the PID controller and neural structure. In this paper, performance of controller which online learning, has been studied adaptive PID controllers, and by experimental study and finally conclusion.

The PIDNN shown in Figure 7, it has three layers consists of a 2-3-1 structure, which are input layer, hidden layer and output layer. The input layer has two neurons, the hidden layer has three and the output layer has only one. The neurons in the net are proportional (P) neuron, integral (I) neuron and derivative (D) neurons.

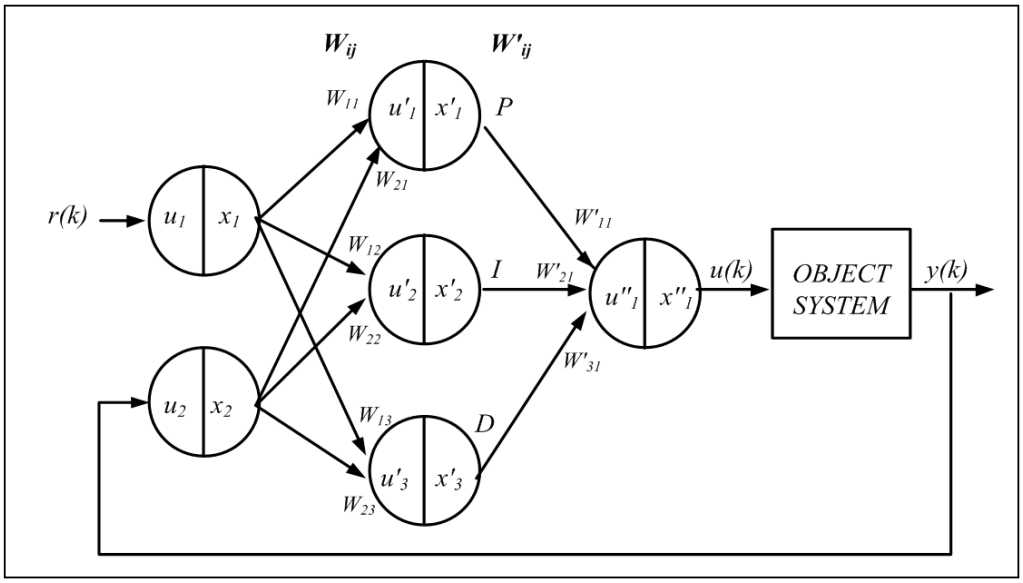

FIGURE 7. Back-propagation algorithms in PIDNN control system

In the input layer, the two output values of the P neuron are calculated form:

$$x_i(k) = \begin{cases} q' & u_i(k) \geq q \\ u_i(k) & -q \leq u_i(k) \leq q \\ -q' & u_i(k) \leq -q \end{cases} \tag{2}$$

where, $i = 1, 2$, is the input number and k is the sample time. The q is maximum limitation value of the input layer and q' is the actual output value after the input value exceeds q. Then, $x_i(k)$ and $u_i(k)$ are the respective input and output values of the i neuron at the k sample time. In the hidden layer, the neurons' inputs are defined as:

$$u'_j(k) = \sum_{i=1}^{2} w_{ij} \cdot x_i(k) \tag{3}$$

where, $j = 1, 2, 3$ and w_{ij} are the connective weight values from input layer. The input-output functions of the P, I, D neurons in the hidden layer are different from each other and different output value of the P-neuron is calculated from:

$$x'_1(k) = \begin{cases} q' & u'_1(k) > q \\ u'_1(k) & -q \leq u'_1(k) \leq q \\ -q' & u'_1(k) < -q \end{cases} \tag{4}$$

The output value of the I-neuron is calculated from:

$$x'_2(k) = \begin{cases} q' & u'_2(k) > q \\ u'_2(k-1) + u'_2(k) & -q \leq u'_2 \leq q \\ -q' & u'_2(k) < -q \end{cases} \tag{5}$$

The output value of the D-neuron is calculated from:

$$x_3'(k) = \begin{cases} q' & u_3'(k) > q \\ u_3'(k) - u_3'(k-1) & -q \le u_3' \le q \\ -q' & u_3'(k) < -q \end{cases} \tag{6}$$

In the output layer, the input of the only P-neuron is defined as:

$$u_h'' = \sum_{j=1}^{3} w_{jh} \cdot x_j'(k) \tag{7}$$

where $h = 1$, is the output number and w_{jh} are the connective values between the hidden and output layers. The input-output function is defined as flows:

$$x_h''(k) = \begin{cases} q' & u_h''(k) > q \\ u_h''(k) & -q \le u_h''(k) \le q \\ -q' & u_h''(k) < -q \end{cases} \tag{8}$$

3.2. **DMFC indirect voltage-mode controller.** Figure 8 shows the voltage-mode control, the V_{FC} is DMFC stack output voltage, battery voltage is $V_{Battery}$ and V_{Load} is load side voltage. In this block diagram, $V_{Battery}$ is regulated and the V_{FC} is controlled indirectly via the dc bus. The V_{FC} is assumed to be regulated by a PIDNN controller by the adjustment of the V_{Load} and battery state of charge. If higher demand of the load leads to larger voltage drop, the V_{FC} is regulated by the bidirectional direct-connected switching interfacing the battery. Therefore, the V_{Load} should be in order to feed a voltage source dc bus. There are two variables that can be used as control inputs, namely load shift (ℓ) and duty cycle (D). PIDNN of control schemes can be realized.

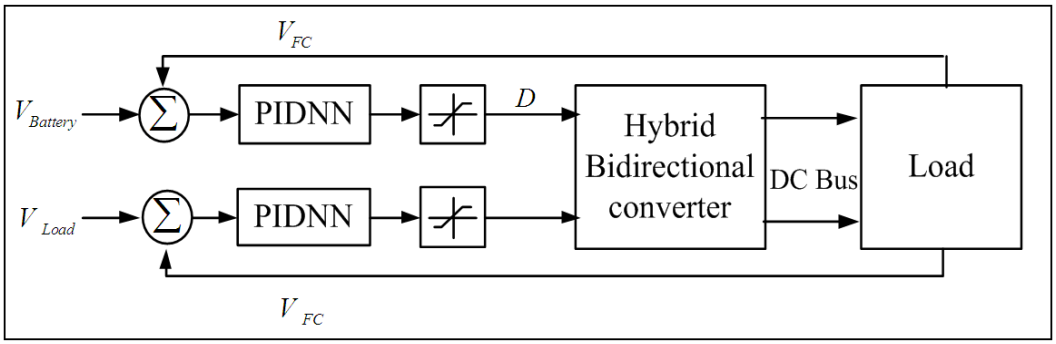

FIGURE 8. Block diagram of PIDNN control

In PIDNN multivariable control system, the aim of the PIDNN algorithms is to minimize

$$I_{FC}J = \sum_{h=1}^{n} E_h = \frac{1}{m} \sum_{h=1}^{n} \sum_{h=1}^{m} [r_h(k) - y_h(k)]^2 \tag{9}$$

where $r_h(k)$ is the inputs and $y_h(k)$ is the outputs of the system, h $(= 1, 2, \ldots, n)$ is the serial number and m is the sampling points in every step. The weight of PIDNN is changed by gradient algorithms in on-line training process. After η training steps, the weights from hidden layer to output layer are

$$w_{sjh}(n+1) = w_{sjh}(n) - \eta \frac{\partial J}{\partial w_{sjh}} \tag{10}$$

where η is the training step, h $(= 1, 2, \ldots, n)$ output neurons' serial number, j $(= 1, 2, 3)$ is the hidden neurons' serial number in every sub-net, s $(= 1, 2, \ldots, n)$ is the sub-nets'

serial number. For hybrid DMFC stack system design, using our proposed control for the battery can be easier than the traditional power control design.

4. **Experimental Results and Discussion.** The proposed control scheme is validated on a hardware prototype experimental setup of the system and experiment environment as show in Figure 9. Taking the operation of electronic load into consideration, the time responses of $V_{FC}(t)$, $I_{FC}(t)$, $I_{Battery}(t)$, $I_{Load}(t)$ and $D(t)$ measured by the DAQ control board are demonstrated in Figure 10. At a low load operation for 20 minutes, the DMFC stack has provided a sufficient current to the load. Thus, the battery SOC is rechargeable and not need to supply any current for the load (see Figure 10(a)). Under such condition, $D(t)$ is controlled as 80% by the PIDNN rules control shown in Figure 10(e). With increasing the load, the $I_{FC}(t)$ will increase but $I_{FC}(t)$ decrease. However, as the required current of the load is higher than 4A, the DMFC stack may run at diffusion region with limited voltage. Consequently, Figure 10(b) shows that the PIDNN control decrease the $D(t)$ (see Figure 10(e)) and $I_{Battery}(t)$ is also increased, then the $V_{FC}(t)$ is hold at limited voltage with 8 V.

Moreover, as hybrid DMFC system operates for 30 minutes later, the significant current drop of $I_{FC}(t)$ is observed in Figure 10(c). This phenomenon is due to the slower reaction of DMFC stack which cannot provide a sufficient current at transient state for high load with 6A requirement. Meanwhile, to balance the output current requirement, the $I_{Battery}(t)$ and $D(t)$ are adjusted to increase by using PIDNN control shown in Figures 10(c) and 10(d), respectively. When considering the dynamics load shown in Figure 10(a), the $V_{FC}(t)$ is controlled successfully within the suitable region (see Figure 10(b)). Finally, the result clearly demonstrates that the $I_{Battery}(t)$ control scheme can stably adjust the shown in Figure 10(d) with varying the $D(t)$ (see Figure 10(e)) during the operation of electronic load.

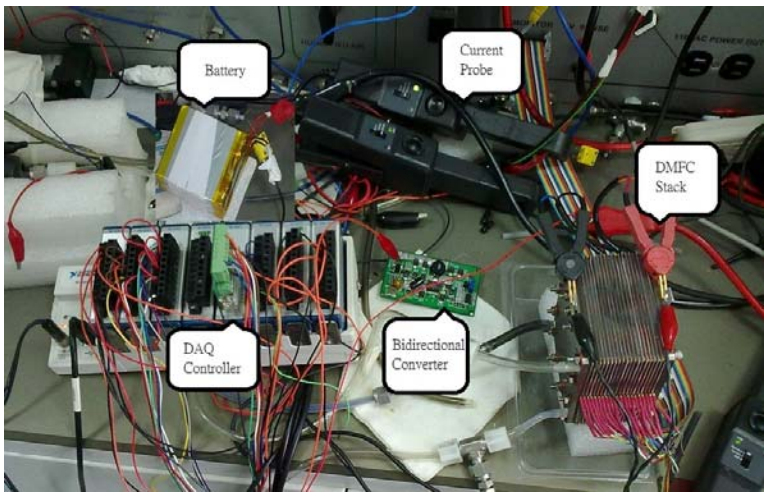

FIGURE 9. Experimental setup environment

5. **Conclusions.** In the hybrid power system, the DMFC and battery power are employed for energy management. In the high load operating mode, the output of the DMFC system provides auxiliary power to help power the battery on the high load as needed. In the low-load operation mode, the hybrid method, whereby extra energy can be stored in the battery, the battery residual energy is also increased due to recharging in response to high load when required next. However, in practice, in regard to the electronic products in the operating mode of the switch, the power consumption will change

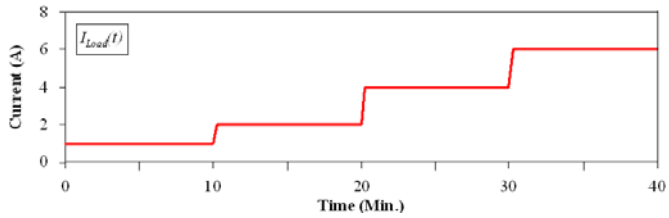

(a)

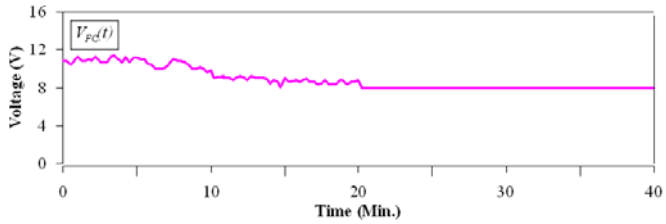

(b)

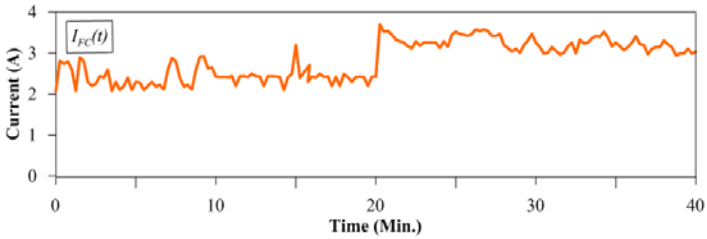

(c)

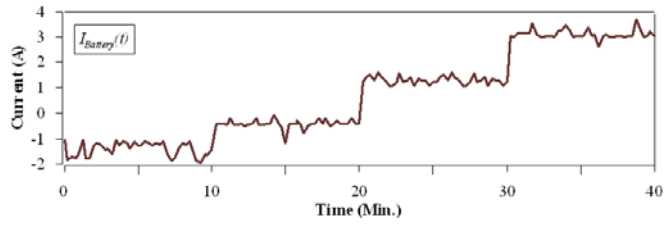

(d)

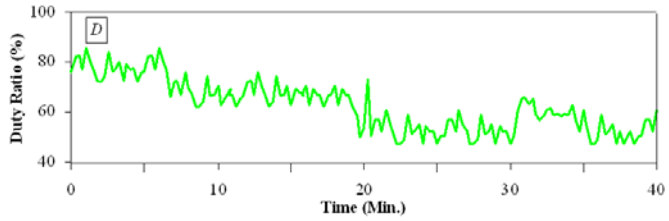

(e)

FIGURE 10. The time responses of (a), (b), (c), (d) and (e), respectively

with the load, switching from standby to full load output or peak load output mode, with the power demand from 10 to 100% between changes. However, the actual power output of DMFC-based backup battery SOC (State Of Charge), to determine the status of the backup battery power saturation, battery backup power cannot increase the output efficiency because of excessive compensation, resulting in DMFC cell stack power output which cannot achieve optimal efficiency. When the backup battery power is at low status, the energy needed to charge the battery (Recharge) is supplied, while the DMFC cell stack, in addition to supplying the load (even for a spare battery outside of the energy pack), so that the output conditions have a huge gain and load requirements due to the lack of an adequate energy supply, which leads to job insecurity, and even causes failure. Furthermore, the mixed-power supply mode, such as the management, cannot be active, making it easy to keep a spare battery in a very short period of time, the repeated charge and discharge of discrete actions; that caused more than the DMFC of backup battery life is short, become another a cost of wear and tear. If the reaction time circuit switching system requirements load slowly (at low load operation after the next detected peak load response for switching), this will more likely result in improper operation with the DMFC causing permanent damage. This paper discusses the control method of the Bidirectional converter for the DMFC/Battery, an active control of hybrid stationary voltage application. Comparing the experimental results shows that the proposed system not only improves the dynamic response of the fuel cell system, but can also significantly compensate for the voltage drop of the fuel cell system due to load changes. The active control can maximize the power produced by the DMFC stack in stable operation when the load is high. The active control can keep the power produced when the load is low for recharging the battery. PIDNN not only has P-neurons but also I-neurons and D-neurons in its hidden layers. PIDNN is a dynamic multilayer network because of its P, I and D neurons and is suitable for control multivariable temperature systems. The PIDNN can handle decoupling and control by a training and self-learning process based on the DMFC fuel cell system. The PIDNN control model and Bidirectional converter can provide a good platform to design a suitable power converter control system for fuel cell system applications.

Acknowledgment. The authors would like to thank the Institute of Nuclear Energy Research (INER) for financially supporting this research.

REFERENCES

[1] J. Ge and H. Liu, Experimental studies of a direct methanol fuel cell, *J. Power Sources*, vol.142, pp.56-69, 2005.

[2] J. Larminie and A. Dicks, *Fuel Cell Systems Explained*, John Wiley and Sons Ltd, Chichester, West Sussex, UK, 2000.

[3] C. Y. Du, T. S. Zhao and W. W. Yang, Effect of methanol crossover on the cathode behavior of a DMFC: A half-cell investigation, *Electrochimica Acta*, vol.52, pp.5266-5271, 2007.

[4] T. Schultz, S. Zhou and K. Sundmacher, Current status of and recent developments in the direct methanol fuel cell, *Chemical Engineering and Technology*, vol.24, pp.1223-1233, 2001.

[5] J. Ge and H. Liu, Experimental studies of a direct methanol fuel cell, *J. Power Sources*, vol.142, pp.56-69, 2005.

[6] B. Gurau and E. S. Smotkin, Methanol crossover in direct methanol fuel cells: A link between power and energy density, *J. Power Sources*, vol.112, pp.339-352, 2002.

[7] Z. Jiang and R. A. Doudal, A compact digitally controlled fuel cell/battery hybrid power source, *IEEE Transactions on Industrial Electronics*, vol.53, no.4, pp.1094-1104, 2006.

[8] T. B. Atwater, P. J. Cygan and F. C. Leung, Man portable power needs of the 21st century: I. Applications for the dismounted soldier. II. Enhanced capabilities through the use of hybrid power sources, *J. Power Sources*, vol.91, no.1, pp.27-36, 2000.

[9] J. P. Meyers and J. Newman, Simulation of the direct methanol fuel cell: II, *J. Electrochem. Soc.*, vol.149, pp.A718-A728, 2002.
[10] Z. Jiang, L. Gao and R. A. Dougal, Design and experimental tests of control strategies for active hybrid fuel cell/battery power sources, *J. Power Sources*, vol.130, no.1, pp.163-171, 2004.
[11] B. Thorstensen, A parametric study of fuel cell system efficacy under full and part load operation, *J. Power Sources*, vol.92, no.1-2, pp.9-16, 2001.
[12] J. P. Zheng, T. R. Jow and M. S. Ding, Hybrid power sources for pulsed current applications, *IEEE Trans. Aerospace and Electronic Sys.*, vol.37, no.1, pp.288-292, 2001.
[13] Y. Choi, N. Chang and T. Kim, DC-DC converter-aware power management for battery-operated embedded systems, *Pro. of the 42nd DAC*, pp.895-900, 2005.
[14] M. J. Khan and M. T. Labal, Modeling and analysis of electro chemical, thermal, and reactant flow dynamics for a PEM fuel cell system, *Fuel Cells*, vol.5, no.4, pp.463-475, 2005.
[15] M. Serra, J. Auado, X. Ansede and J Riera, Controllability analysis of decentralized linear controllers for polymeric fuel cells, *J. Power Sources*, vol.151, pp.93-102, 2005.
[16] B.-D. Lee, D.-H. Jund and Y.-H. Ko, Analysis of DMFC/battery hybrid power system for portable applications, *J. Power Sources*, vol.131, pp.207-212, 2004.
[17] J. Han and E.-S. Park, Direct methanol fuel-cell combined with a small backup battery, *J. Power Sources*, vol.112, pp.477-483, 2002.
[18] L. Gao, Z. Jiang and R. A. Dougal, An actively controlled fuel cell/battery hybrid to meet pulsed power demands, *J. Power Sources*, vol.130, no.2, pp.202-207, 2004.
[19] W. U. Huynh, J. J. Dittmer and A. P. Alivisatos, Hybrid nanorod-polymer solar cells, *Science*, vol.295, no.5564, pp.2425-2427, 2002.
[20] W. Gao, Performance comparison of a fuel cell-battery hybrid powertrain and a fuel cell-ultracapacitor hybrid powertrain, *Proc. of the IEEE Transactions on Vehicular Technology*, vol.54, no.3, pp.846-855, 2005.
[21] Z. Jiang and R. A. Dougal, A compact digitally controlled fuel cell/battery hybrid power source, *Proc. of the IEEE Transactions on Industrial Electronics*, vol.53, no.4, pp.1094-1104, 2006.
[22] M. Nadal and F. Barbir, Development of a hybrid fuel cell/battery powered electric vehicle, *International Journal of Hydrogen Energy*, vol.21, no.6, pp.497-505, 2006.
[23] K.-S. Jeong, W.-Y. Lee and C.-S. Kim, Energy management strategies of a fuel cell/battery hybrid system using fuzzy logics, *J. Power Sources*, vol.145, no.2, pp.319-326, 2005.
[24] S. Rosiek and F. J. Batlles, Modelling a solar-assisted air-conditioning system installed in CIESOL building using an artificial neural network, *Renewable Energy*, vol.35, no.12, pp.2894-2901, 2010.
[25] E. A. Mohamed, H. A. Talaat and E. A. Khamis, Fault diagnosis system for tapped power transmission lines, *Electric Power Systems Research*, vol.80, no.5, pp.599-613, 2010.
[26] M. Matsubara, Y. Usui and S. Sugimoto, Identification of continuous-time MIMO systems via sampled data, *International Journal of Innovative Computing, Information and Control*, vol.2, no.5, pp.1119-1136, 2006.
[27] C. Shi and G. Zhang, A new method of PID control based on improved BP neural network, *Control Conference*, pp.1167-1171, 2007.
[28] H. Shu and Y. Pi, PID neural networks for time-delay systems, *Computers and Chemical Engineering*, vol.24, pp.859-862, 2000.
[29] H. L. Shu and L. Shu, PID neural network in multivariable time-varying systems, *Dynamics of Continuous Discrete and Impulsive Systems – Series B: applications and Algorithms*, vol.2, pp.822-824, 2005.
[30] H. Shu and X. Guo, Decoupling control of multivariable time-varying systems based on PID neural network, *Proc. of the 5th Asian Control Conference*, vol.1, pp.682-685, 2004.
[31] Y. Wakasa, K. Tanaka, T. Akashi and Y. Nishimura, PSO-based simultaneous tuning method for PID controllers and dead-zone compensators and its application to ultrasonic motors, *International Journal of Innovative Computing, Information and Control*, vol.6, no.10, pp.4593-4604, 2010.
[32] G.-D. Li, S. Masuda, D. Yamaguchi and M. Nagai, The optimal GNN-PID control system using particle swarm optimization algorithm, *International Journal of Innovative Computing, Information and Control*, vol.5, no.10(B), pp.3457-3469, 2009.
[33] Y. Abe, M. Konishi and J. Imai, Neural network based diagnosis system for looper height controller of hot strip mills, *International Journal of Innovative Computing, Information and Control*, vol.3, no.4, pp.919-935, 2007.